

# Chiral Edge Fluctuations of Colloidal Membranes

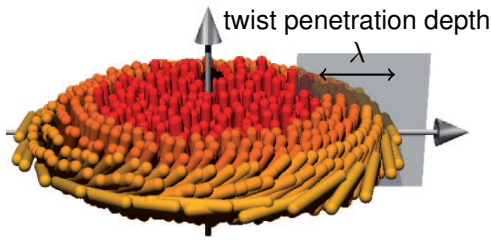
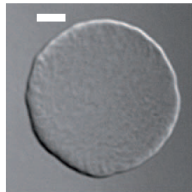
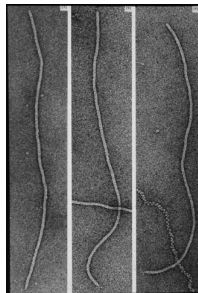
**Leroy Jia** (w/ T. Powers & R. Pelcovits)

SIAM Conference on the Life Sciences

August 6, 2018



# Colloidal membranes are composed of rod-like viruses



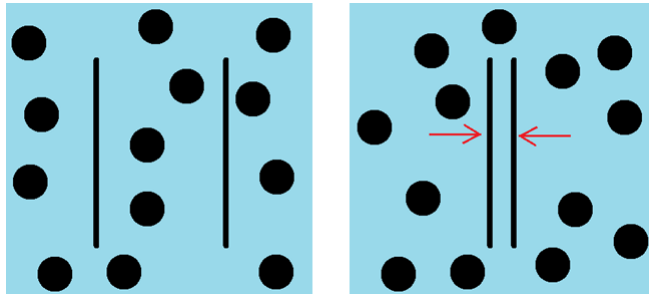
- Left: *fd* virus<sup>1</sup>, 870 nm × 6 nm
- Center: DIC image<sup>2</sup>, scale bar = 5 μm
- Right: Color indicates angle relative to normal<sup>2</sup>

<sup>1</sup>Model and Russel, *The Bacteriophages*. R.New York:Plenum (1988)

<sup>2</sup>Gibaud et. al, *Nature* **481**, 348 (2012)

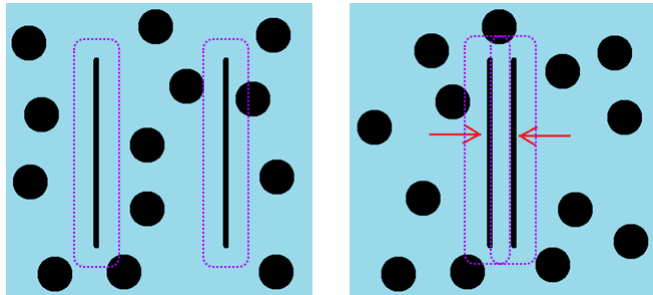
# Polymer depletant induces attractive forces

First described by Asakura and Oosawa (1954)



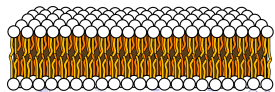
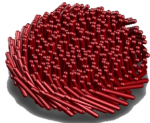
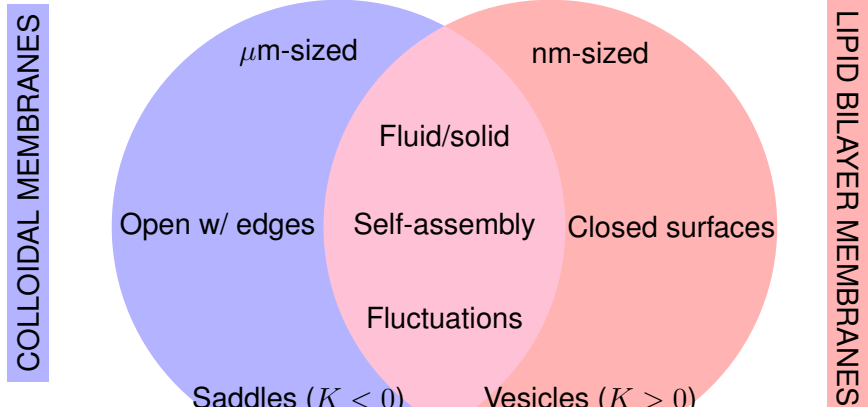
# Polymer depletant induces attractive forces

First described by Asakura and Oosawa (1954)



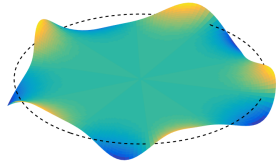
$$F = -Nk_B T \log(V - V_{ex}) \simeq nk_B T V_{ex}$$

# Colloidal membranes are familiar and different

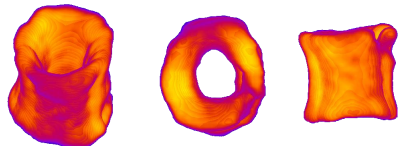


# Colloidal membranes exhibit diverse phenomena

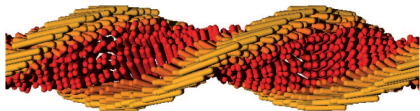
Chiral edge fluctuations



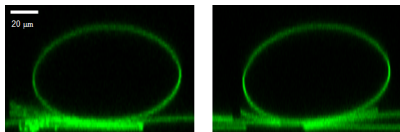
Unduloid formation



Ribbon force vs. extension

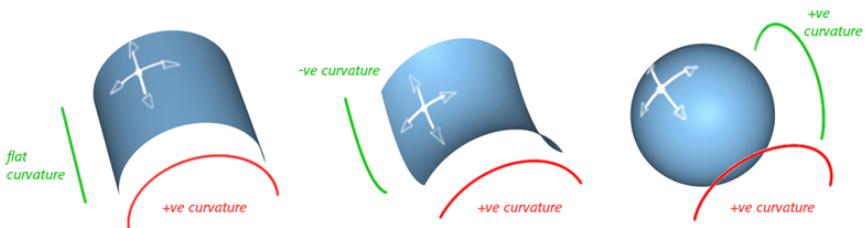


Colloidal vesicles



# Canham-Helfrich energy models membrane bending

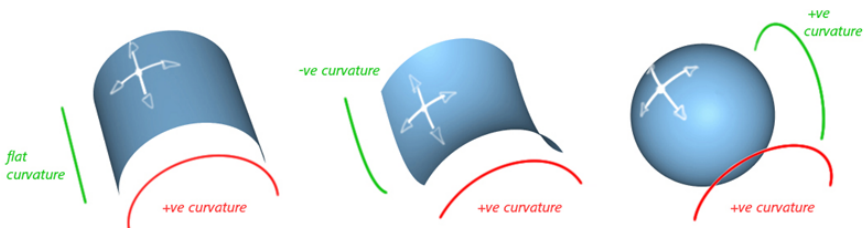
$$E_{CH} = \frac{\kappa}{2} \int (2H)^2 dA + \bar{\kappa} \int K dA + \mu \int dA$$



# Canham-Helfrich energy models membrane bending

$$E_{CH} = \frac{\kappa}{2} \int (2H)^2 dA + \bar{\kappa} \int K dA + \mu \int dA$$

- Mean curvature ( $\kappa \sim 10^5 k_B T$ )



# Canham-Helfrich energy models membrane bending

$$E_{CH} = \frac{\kappa}{2} \int (2H)^2 dA + \bar{\kappa} \int K dA + \mu \int dA$$

curvature ( $\kappa \sim 10^5 k_B T$ )      ↗  
 mean curvature ( $\bar{\kappa} \sim 10^2 k_B T$ ) ↘

- Mean curvature ( $\kappa \sim 10^5 k_B T$ ) /
  - Gaussian curvature ( $\bar{\kappa} \sim 10^2 k_B T$ )

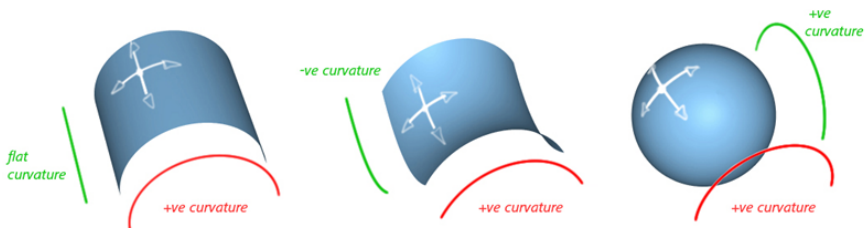
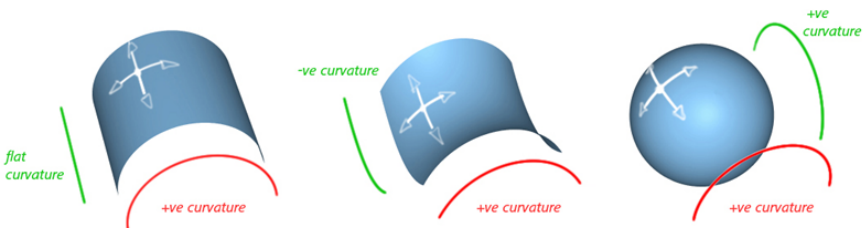


*Image:* Website, Autodesk Alias Workbench

# Canham-Helfrich energy models membrane bending

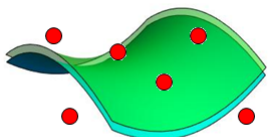
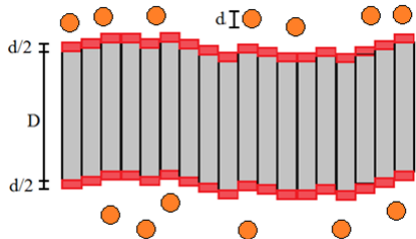
$$E_{CH} = \frac{\kappa}{2} \int (2H)^2 dA + \bar{\kappa} \int K dA + \mu \int dA$$

- Mean curvature ( $\kappa \sim 10^5 k_B T$ )
- Gaussian curvature ( $\bar{\kappa} \sim 10^2 k_B T$ )
- Lagrange multiplier



# Entropy favors positive Gaussian curvature modulus

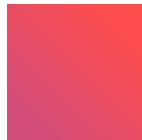
$$V_{ex} \approx D \int dA + \frac{D^2 d}{4} \int K dA$$



$$\bar{\kappa} = \frac{1}{4} n k_B T D^2 d + \bar{\kappa}_{in} \approx 200 k_B T$$

# Line tension limits membrane perimeter

$$E_{LT} = \gamma \int ds$$



$\gamma$  can depend on

- depletant concentration
- temperature
- chirality

# Frank energy models liquid crystalline (LC) order

$$E_F = \frac{1}{2} \int \left[ K_1(\nabla \cdot \hat{n})^2 + K_2(\hat{n} \cdot (\nabla \times \hat{n}) - q)^2 + K_3(\hat{n} \times (\nabla \times \hat{n}))^2 + C \sin^2 \theta \right] dA$$

The diagram illustrates three types of liquid crystal distortions:

- a splay**: The director field (red ellipsoids) is tilted away from the normal of the blue plates.
- b twist**: The director field rotates continuously from one plate to the other.
- c bend**: The director field is curved within the plane of the plates.

Image: S. Copar, *Physics Reports* 538, 1 (2014)

# Frank energy models liquid crystalline (LC) order

$$E_F = \frac{1}{2} \int \left[ K_1(\nabla \cdot \hat{n})^2 + K_2(\hat{n} \cdot (\nabla \times \hat{n}) - q)^2 + K_3(\hat{n} \times (\nabla \times \hat{n}))^2 + C \sin^2 \theta \right] dA$$

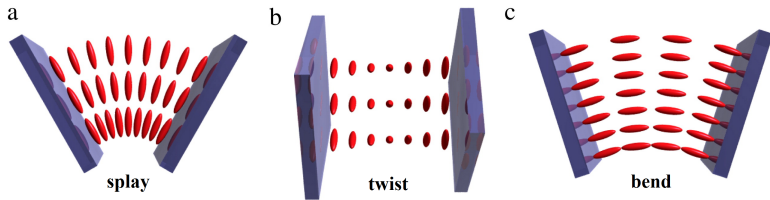
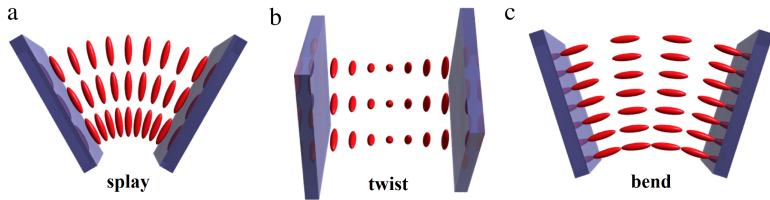


Image: S. Copar, *Physics Reports* 538, 1 (2014)

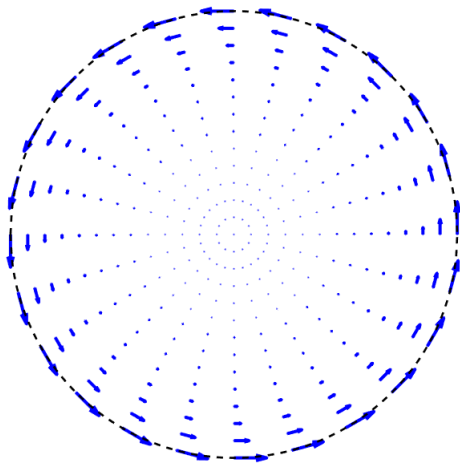
# Frank energy models liquid crystalline (LC) order

$$E_F = \frac{1}{2} \int \left[ K_1(\nabla \cdot \hat{n})^2 + K_2(\hat{n} \cdot (\nabla \times \hat{n}) - q)^2 + K_3(\hat{n} \times (\nabla \times \hat{n}))^2 + C \sin^2 \theta \right] dA$$

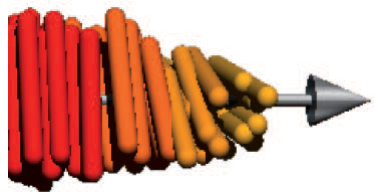
- $\sqrt{K_2/C}$  defines the twist penetration depth  $\lambda$



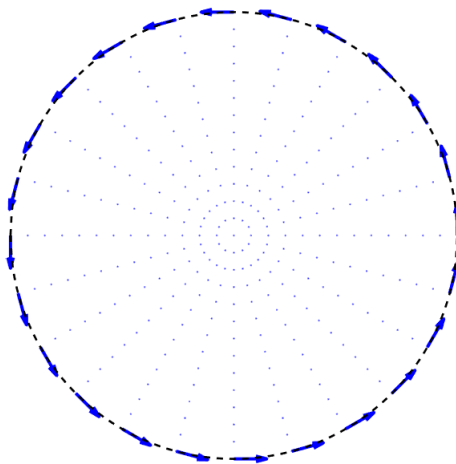
# An effective term accounts for the LC bend



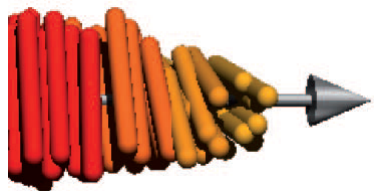
$$\theta \sim \frac{\pi}{2} \exp\left(-\frac{a-r}{\lambda}\right)$$



# An effective term accounts for the LC bend

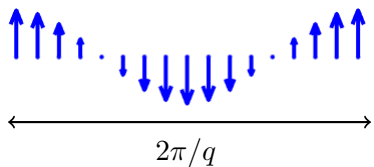


$$\frac{K_3}{2} \int (\hat{n} \times (\nabla \times \hat{n}))^2 dA \simeq \frac{B}{2} \int k^2 ds$$



# An effective term accounts for the LC twist

The chirality  $q$  is represented as an inherent geodesic torsion  $\tau_g^*$ .

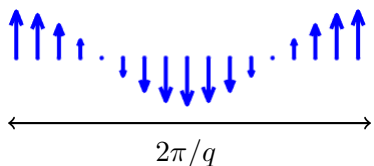


$$\tau_g = \hat{t} \cdot \left( \hat{N} \times \frac{d\hat{N}}{ds} \right) = q$$

$$\frac{K_2}{2} \int (\hat{n} \cdot (\nabla \times \hat{n}) - q)^2 dV \simeq \frac{B'}{2} \int (\tau_g - \tau_g^*)^2 ds$$

# An effective term accounts for the LC twist

The chirality  $q$  is represented as an inherent geodesic torsion  $\tau_g^*$ .



$$\tau_g = \hat{t} \cdot \left( \hat{N} \times \frac{d\hat{N}}{ds} \right) = q$$

$$\frac{K_2}{2} \int (\hat{n} \cdot (\nabla \times \hat{n}) - q)^2 dV \simeq \frac{B'}{2} \int (\tau_g - \tau_g^*)^2 ds$$

We define the effective chirality modulus  $c^* = -B' \tau_g^*$ .

# Membrane shapes are found by minimizing energy

$$E = \int_S \left[ \frac{\kappa}{2} (2H)^2 + \bar{\kappa} K + \mu \right] dA + \int_{\partial S} \left[ \gamma + \frac{B}{2} k^2 + \frac{B'}{2} \tau_g^2 + c^* \tau_g \right] ds$$

<sup>3</sup>Website, "The geometry of soap films and soap bubbles"

<sup>4</sup>Website, "An ant rolling a sphere of water across the surface of a garden pond"

<sup>5</sup>Website, "Willmore Day at Durham" (Blog of Kevin Houston)

# Membrane shapes are found by minimizing energy

$$E = \int_S \left[ \frac{\kappa}{2} (2H)^2 + \bar{\kappa} K + \mu \right] dA + \int_{\partial S} \left[ \gamma + \frac{B}{2} k^2 + \frac{B'}{2} \tau_g^2 + c^* \tau_g \right] ds$$

Euler-Lagrange equation:

$$\kappa(\nabla^2 H + 2H^3 - 2HK) - \mu H = 0$$

---

<sup>3</sup>Website, "The geometry of soap films and soap bubbles"

<sup>4</sup>Website, "An ant rolling a sphere of water across the surface of a garden pond"

<sup>5</sup>Website, "Willmore Day at Durham" (Blog of Kevin Houston)

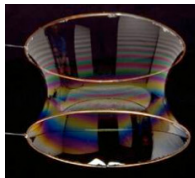
# Membrane shapes are found by minimizing energy

$$E = \int_S \left[ \frac{\kappa}{2} (2H)^2 + \bar{\kappa} K + \mu \right] dA + \int_{\partial S} \left[ \gamma + \frac{B}{2} k^2 + \frac{B'}{2} \tau_g^2 + c^* \tau_g \right] ds$$

Euler-Lagrange equation:

$$\kappa(\nabla^2 H + 2H^3 - 2HK) - \mu H = 0$$

Solutions: minimal surfaces<sup>3</sup>, CMC surfaces<sup>4</sup>, Willmore surfaces<sup>5</sup>



<sup>3</sup>Website, "The geometry of soap films and soap bubbles"

<sup>4</sup>Website, "An ant rolling a sphere of water across the surface of a garden pond"

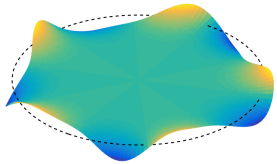
<sup>5</sup>Website, "Willmore Day at Durham" (Blog of Kevin Houston)

# Outline

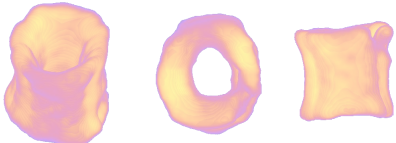
## 0. Motivation and mathematical model

### I. Chiral edge fluctuations

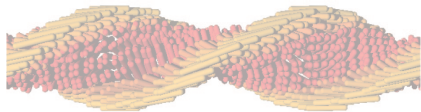
w/ M. J. Zakhary, Z. Dogic, R. A. Pelcovits, and T. R. Powers



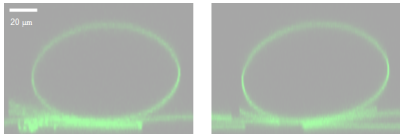
### II. Unduloids



### III. Force vs. extension



### IV. Colloidal vesicles



# Temperature quench induces disk-to-ribbon transition

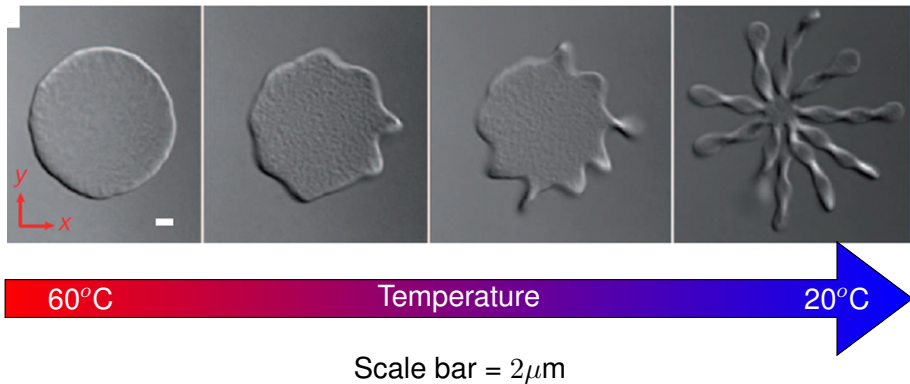
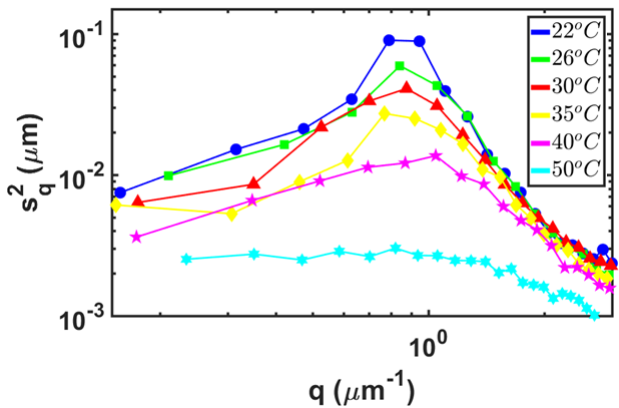
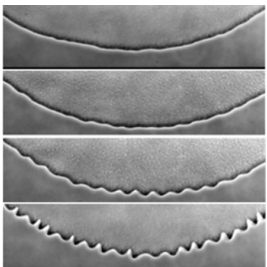


Image: Gibaud et. al, *Nature* **481**, 348 (2012)

# Edge fluctuation spectrum exhibits an anomalous peak



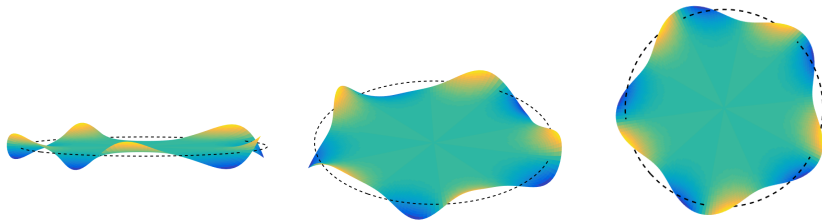
$$\langle s_q^2 \rangle = \frac{k_B T}{Bq^2 + \gamma}$$



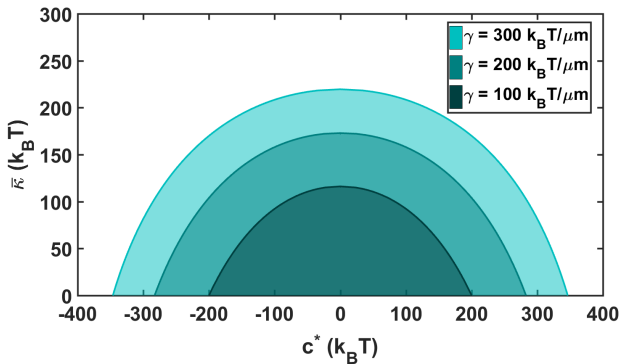
# Perturb a disk with a helical ripple

$$E_{flat} = 2\pi R\gamma + \frac{B\pi}{R}$$

$$E = \int_{\mathcal{S}} \left[ \frac{\kappa}{2} (2H)^2 + \bar{\kappa} K + \mu \right] dA + \int_{\partial\mathcal{S}} \left[ \gamma + \frac{B}{2} k^2 + \frac{B'}{2} \tau_g^2 + c^* \tau_g \right] ds$$



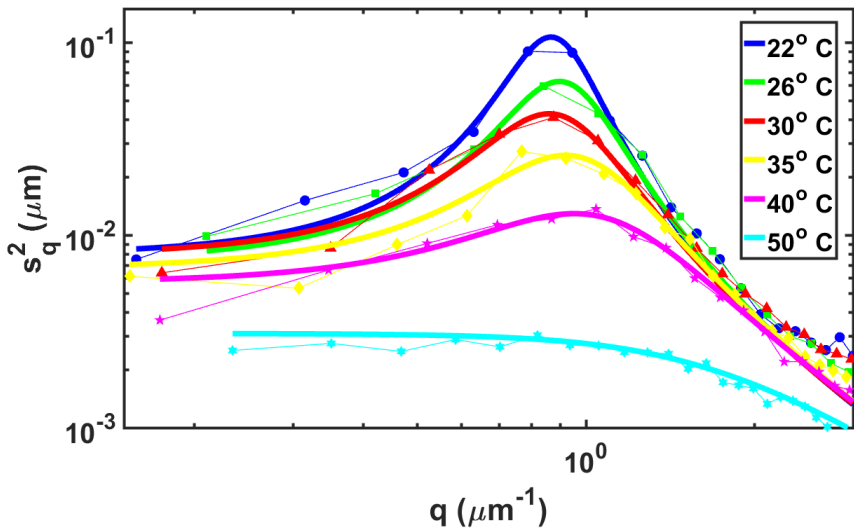
Flat membrane is unstable when  $c^*$  or  $\bar{\kappa}$  is large



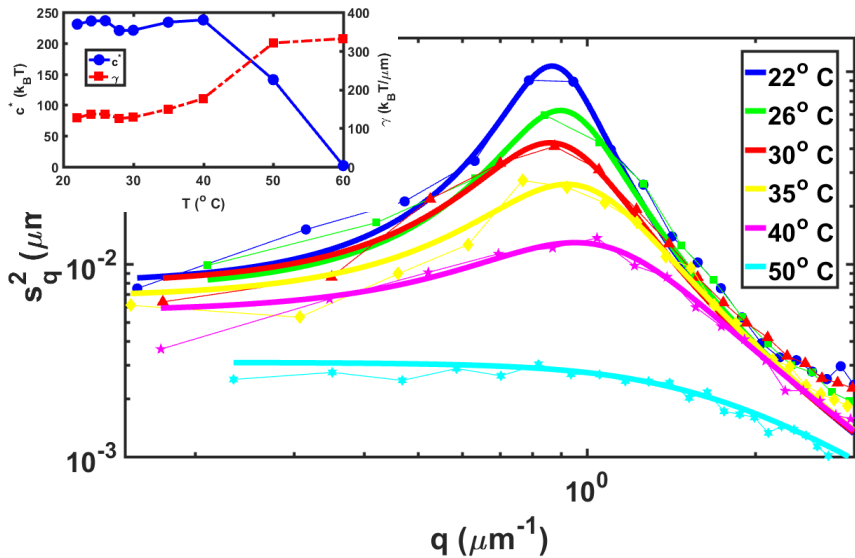
$$\langle u_q^2 \rangle = \frac{k_B T}{Bq^4 + \gamma q^2 - c^{*2} q^4 / (2Bq^2 + \gamma - 2\bar{\kappa}|q|)}$$

$$\langle v_q^2 \rangle = \frac{k_B T}{2Bq^4 + \gamma q^2 - 2\bar{\kappa}|q|^3 - c^{*2}q^4/(Bq^2 + \gamma))}$$

# Peak forms near instability with chirality



# Peak forms near instability with chirality



# Conclusion

- Out-of-plane fluctuation spectrum displays an anomalous peak in chiral samples
- Peak corresponds to onset of instability and grows as chirality and/or Gaussian curvature modulus increase
- Our **effective model that accounts for liquid crystalline order through geometric properties of the edge** quantifies the coupling of in- and out-of-plane fluctuations to produce the peak

# Acknowledgements



- Tom Powers (ENGN & PHYS)
- Bob Pelcovits (PHYS)



This work was supported by National Science Foundation grants

- **MRSEC DMR-1420382**
- **CMMI-1634552**



- Andrew Balchunas (Brandeis)
- Joanna Robaszewski (Brandeis)
- Prerna Sharma (Indian Institute of Science)
- Mark Zakhary (Mayo Clinic)
- Zvonimir Dogic (UCSB/Brandeis)

We are grateful to the **Brandeis U. MRSEC** for funding and resources.

***Thank you for listening!***